

A Simple Asymmetric Hysteresis Model for Displacement-Force Control of Piezoelectric Actuators

Sepehr Zarif Mansour
Engineering Department, UBC
Kelowna, Canada
sepehr.zmansour@alumni.ubc.ca

Rudolf Seethaler
Engineering Department, UBC
Kelowna, Canada

Andrew Fleming
The University of Newcastle,
Callaghan, Australia

Abstract—This article presents a simple hysteresis model for piezoelectric actuators that can be used for simultaneous displacement-force control applications. The presented model maps the hysteresis voltage of an actuator to the charge passing through it. It can model asymmetric hysteresis loops and does not require to be inverted for real-time implementations.

The presented model consists of two exponential functions which are described by only four parameters that are identified from a single identification experiment. Another advantage of the presented model over the existing models is that, it requires measurements of current rather than charge. A simultaneously varying displacement-force experiment is created to frame the model. An average absolute error value of 8 % for the hysteresis voltage-charge fit is calculated. Consequent displacement and force fits have average absolute error value of 2.5 %, which are similar to the best reported in displacement-force control literature.

Index Terms—Hysteresis model, Piezoelectric actuator, displacement-force control.

I. INTRODUCTION

Piezoelectric actuators are widely employed in precision actuation due to fast response, nanometer-scale resolution, and large operational force [1]. However, they exhibit nonlinearities such as hysteresis, which degrades their performance [2]. A large number of studies in the literature focus on hysteresis compensation under constant force conditions. They employ phenomenological hysteresis models, such as the generalized Maxwell slip model [3], the Prandtl-Ishlinskii model [4], or the Preisach model [5].

These hysteresis models, first use a calibration experiment to map the driving voltage of an actuator to its displacement. The map is then inverted for calculating the feed forward voltage required for a desired displacement [4]. Inverting the generalized Maxwell slip and the original Prandtl-Ishlinskii models is straightforward. However, they are not able to model asymmetric displacement-voltage profiles [6]. Consequently the Prandtl-Ishlinskii hysteresis model has been modified to take asymmetry into account [7]. This modification however, adds extra computation to the real time implementation of the model. The Preisach model is

able to model asymmetric hysteresis; However, inverting the Preisach model is computationally expensive [6].

For non constant force conditions, the same phenomenological hysteresis models with their associated inversion procedures can be used to model the voltage-charge hysteretic profile [2], [8]. However, the large number of hysteresis operators required for accurately describing voltage-charge hysteresis are extremely computationally expensive. [6].

This article presents a new asymmetric hysteresis model for simultaneous displacement-force control applications. Real-time implementation of the presented model is simpler than conventional models, since it requires much less mathematical operations; it is described by only four parameters, which are determined via a single calibration experiment. Further, in contrast to conventional phenomenological models, the presented model does not need to be inverted. The remainder of the paper is organized as follows.

Section II reviews the constitutive equations governing piezoelectric actuators. Section III describes the experiments. The new hysteresis model is framed in Section IV. Conclusions are provided in Section V.

II. THE ELECTROMECHANICAL MODEL OF PIEZOELECTRIC ACTUATORS

This section first describes the constitutive equations that govern piezoelectric actuators. These equations are then employed to explain the characteristics of the proposed hysteresis model for simultaneous displacement-force control applications.

A. Constitutive Equations

Goldfarb and Celanovic presented a lumped parameter model that describes the relationships between the displacement x , external force F , driving voltage V_d , and electrical charge q passing through a piezoelectric actuator taking the hysteresis nonlinearity into account [9]. The mathematical representation of the model for quasi-static applications is

$$V_d = V_p + V_h, \quad (1)$$

$$V_h = H(q), \quad (2)$$

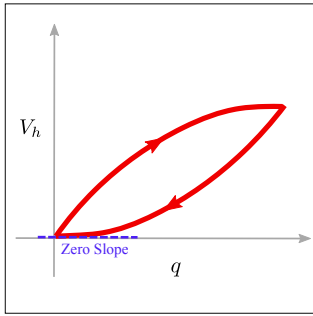


Fig. 1: A qualitative representation of the parameter identification criteria used in [2], [6]: the descending branch of the V_h - q hysteresis loop must have zero slope at the end of the branch.

$$kx = F + \alpha V_p, \quad (3)$$

$$q = \alpha x + C_p V_p, \quad (4)$$

where, k is the stiffness, C_p is the clamped capacitance of the actuator, and α is a piezoelectric constant that links the electrical domain to the mechanical domain.

The driving voltage V_d in (1) consists of a linear voltage V_p and a nonlinear hysteresis voltage V_h . Equation (2) suggests that the hysteresis voltage is purely a function of charge. The corresponding hysteresis function is represented as H . Displacement, external force, and the generated piezoelectric force αV_p are linked via (3). Equation (4) indicates that the charge passing through the actuator consists of the charge passing through the clamped capacitance and the internal charge generated as a result of the actuator's movement αx .

B. Hysteresis models for displacement-force control applications

The application of constitutive equations (1-4) require the identification of the model parameters, k , α , and C_p as well as the hysteresis model $H(q)$. The parameter identification method in [2] fits experimental data to $q = (\alpha + \frac{C_p k}{\alpha})x - \frac{C_p}{\alpha}F = a_x x + a_F F$ to find the displacement and force coefficients. An additional relationship is then required to uniquely identify k , α , and C_p , from a_x and a_F . Typically the slope at the end of the descending branch of the V_h - q hysteresis loop is set to zero [2], [6] as shown in Figure 1. This method is employed in Section III to identify V_h in a simultaneously varying displacement-force experiment. Section IV then presents a simple hysteresis model that maps V_h to q .

III. EXPERIMENTS

The experimental apparatus for conducting simultaneously varying displacement-force experiments is described in subsection A. The parameter identification method described in Section II is used to identify V_h in subsection B.

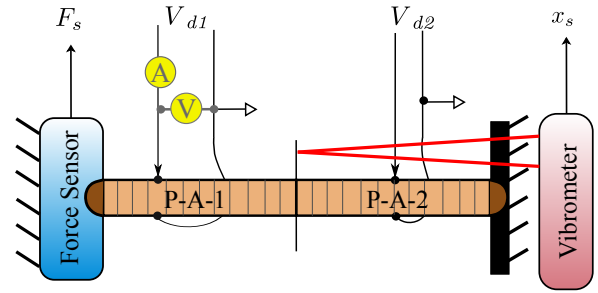


Fig. 2: The experimental apparatus.

A. The experimental apparatus

A two degree of freedom experimental apparatus is employed in this study. It consists of two piezoelectric stack actuators, P-A-1 and P-A-2, assembled in series. The apparatus is depicted in Figure 2. Both actuators are PI-885.90 from Physic Instrumente with maximum free displacements of $32 \mu m$ (at 100 V) and maximum blocked forces of 950 N at (120 V).

By varying driving voltages V_{d1} and V_{d2} , the tip displacement x_s of the actuators and the external force F_s vary independent from each other. Measurements of displacement x_s , Force F_s , driving voltage V_{d1} , and current I_1 are collected for P-A-1. A Polytec-HSV2002 laser vibrometer with a resolution of $0.3 \mu m$ measures x_s . A PCB-208C2 force sensor with a resolution of 4 mN measures F_s . The voltage measurement is carried out via a Tektronix-P2220 voltage probe. Current is measured via a Tektronix-TCPA300 current probe. Charge q_1 passing through P-A-1 is determined via integrating I_1 . A detailed description of the apparatus can be found in [10].

B. The experimental data

A simultaneously varying displacement-force experiment is created using the described experimental apparatus. Figure 3(a) shows the generated force-displacement map. The numbered arrows indicate the sequence of segments traversed

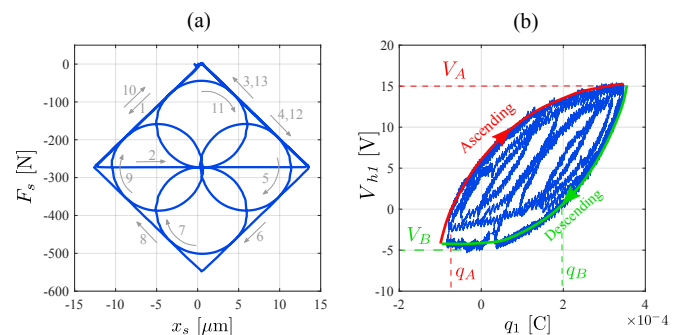


Fig. 3: (a) A simultaneously varying force-displacement map generated using the apparatus in Figure 2. (b) The measured hysteresis voltage (using the parameter identification method in [2]) vs. charge passing through P-A-1.

on the map. Boundaries of the generated map are associated with the voltage limitation of V_{d1} and V_{d2} (0-100 V).

Using the parameter identification method described in [2] and reviewed in Section II, hysteresis voltage of P-A-1 V_{h1} is determined from the measurements of x_s , F_s , V_{d1} , and q_1 . Figure 3(b) shows the resulting V_{h1} - q_1 hysteresis profile. Section IV fits the proposed hysteresis model to the measured V_{h1} - q_1 profile.

IV. A NEW ASYMMETRIC HYSTERESIS MODEL

The proposed hysteresis model consists of two exponential functions, one for ascending branches and one for descending branches of the hysteresis loop as shown in Figure 3(b)

$$\tilde{V}_{h1} = \begin{cases} V_A(1 - e^{-\frac{q_1 - q_A}{\tau_A}}), & \text{if } I_1 \geq 0 \\ V_B(1 - e^{-\frac{q_1 - q_B}{\tau_B}}), & \text{otherwise} \end{cases} \quad (5)$$

where, V_A and V_B are the maximum and minimum values of V_{h1} respectively; τ_A and τ_B are the charge constants of the ascending and descending branches respectively; q_A and q_B are the zero crossings of V_{h1} , which are dependent on the loop reversal points.

To eliminate the need for determining q_A and q_B in the real-time calculation of V_{h1} , (5) and (6) are reformulated using finite differences over the sampling period Δt

$$\tilde{V}_{h1(i)} = \begin{cases} \tilde{V}_{h1(i-1)} + (V_A - \tilde{V}_{h1(i-1)}) \frac{\Delta t}{\tau_A} I_{1(i)}, & \text{if } I_{1(i)} \geq 0. \\ \tilde{V}_{h1(i-1)} + (V_B - \tilde{V}_{h1(i-1)}) \frac{\Delta t}{\tau_B} I_{1(i)}. & \text{otherwise.} \end{cases} \quad (7)$$

An added benefit of this formulation is that it requires measurements of current rather than charge. The starting value for V_h would usually be V_B , since this values corresponds to the de-energized state of the actuator. Model parameters V_A , V_B , τ_A , and τ_B are determined using least square error minimization, where experimental data from ascending branches provide fitted values for V_A and τ_A

$$\begin{bmatrix} V_A \\ \tau_A \end{bmatrix} = \begin{bmatrix} \sum \Delta V_{h1(i)} \Delta t I_{1(i)} & - \sum (\Delta V_{h1(i)})^2 \\ \sum (\Delta t I_{1(i)})^2 & - \sum \Delta V_{h1(i)} \Delta t I_{1(i)} \end{bmatrix}^{-1} \times \begin{bmatrix} \sum V_{h1(i)} \Delta V_{h1(i)} \Delta t I_{1(i)} \\ \sum V_{h1(i)} (\Delta t I_{1(i)})^2 \end{bmatrix}, \quad (8)$$

and data from the descending branches provide fitted values for V_B and τ_B :

$$\begin{bmatrix} V_B \\ \tau_B \end{bmatrix} = \begin{bmatrix} - \sum \Delta V_{h1(i)} \Delta t I_{1(i)} & - \sum (\Delta V_{h1(i)})^2 \\ \sum (\Delta t I_{1(i)})^2 & \sum \Delta V_{h1(i)} \Delta t I_{1(i)} \end{bmatrix}^{-1} \times \begin{bmatrix} - \sum V_{h1(i)} \Delta V_{h1(i)} \Delta t I_{1(i)} \\ \sum V_{h1(i)} (\Delta t I_{1(i)})^2 \end{bmatrix}, \quad (9)$$

where, $\Delta V_{h1(i)} = V_{h1(i)} - V_{h1(i-1)}$. The identified values are summarized in Table I.

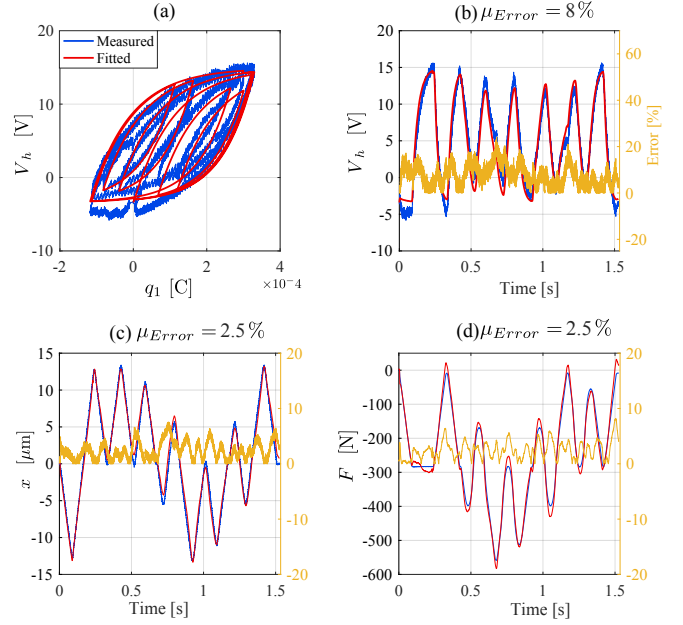


Fig. 4: (a) Measured and fitted hysteresis loops. (b) Measured and fitted hysteresis voltage time signals. (c) Measured and fitted displacement time signals. (d) Measured and fitted force time signals.

TABLE I: Identified parameters for the presented hysteresis model.

Parameter	Identified value
V_A	15.00 V
τ_A	0.11 mC
V_B	-3.84 V
τ_B	0.09 mC

Two different charge constants τ_A and τ_B guarantee that the model is able to represent asymmetry in the hysteresis loops.

The measured and fitting results using the proposed model are depicted in Figure 4. Figure 4(a) depicts the fitted \tilde{V}_{h1} - q_1 hysteresis loop using (7), together with the measured V_{h1} - q_1 hysteresis loop. Figure 4(b) shows the error between \tilde{V}_{h1} and V_{h1} over time. An average absolute error value of $\mu_{Error} = 8\%$ for the fit between \tilde{V}_{h1} and V_{h1} is obtained.

Since the magnitude of the hysteresis voltage is about 15% of the magnitude of the driving voltage, using this hysteresis model would lead to around 2% errors in the estimation of displacement and force using (1-4). This prediction is validated in Figures 4(c) and 4(d), where average absolute error values of $\mu_{Error} = 2.5\%$ for the displacement and force fittings are obtained respectively. These errors are similar to the best reported in the literature [8], [2].

V. CONCLUSION

This article presented a new exponential hysteresis model that can be used for simultaneous displacement-force control applications, where the hysteresis voltage is mapped to the charge.

The presented model consists of two exponential functions which are described by only four parameters that are identified from a single identification experiment. The model does not need to be inverted for real time implementation and is able to model asymmetric hysteresis voltage-charge loops.

An average absolute error value of $\mu_{Error} = 8\%$ for the fit is calculated. Given the fact that the hysteresis nonlinearity is about 15% of the driving voltage used in the experiment, about 2% error is predicted in displacement and force control of the piezoelectric actuators. The expected errors are validated for the displacement and force fits.

Even-though the presented model is not a comprehensive model and only models the hysteresis loops with exponential-shaped branches, its resulting displacement and force errors are similar to the best reported in the literature [1], [8]. Also, its simplicity is highly desirable in real-time implementations.

ACKNOWLEDGMENT

The research was funded by Project Grant 62R82920 from Canadas Natural Sciences and Engineering Research Council.

REFERENCES

- [1] S. Z. Mansour and R. Seethaler, "On the feasibility of using measurements of charge and effective capacitance for simultaneous position and force self-sensing of piezoelectric actuators," in *Advanced Intelligent Mechatronics (AIM), 2016 IEEE International Conference on*. IEEE, 2016, pp. 448–451.
- [2] S. Z. Mansour and R. J. Seethaler, "Simultaneous displacement and force estimation of piezoelectric stack actuators using charge and voltage measurements," *IEEE/ASME Transactions on Mechatronics*, vol. 22, no. 6, pp. 2619–2624, 2017.
- [3] Y. Liu, J. Shan, Y. Meng, and D. Zhu, "Modeling and identification of asymmetric hysteresis in smart actuators: A modified ms model approach," *IEEE/ASME Transactions on Mechatronics*, vol. 21, no. 1, pp. 38–43, 2016.
- [4] K. Kuhnen and H. Janocha, "Inverse feedforward controller for complex hysteretic nonlinearities in smart-material systems," *Control and Intelligent systems*, vol. 29, no. 3, pp. 74–83, 2001.
- [5] A.-F. Boukari, J.-C. Carmona, G. Moraru, F. Malburet, A. Chaaba, and M. Douimi, "Piezo-actuators modeling for smart applications," *Mechatronics*, vol. 21, no. 1, pp. 339–349, 2011.
- [6] A. Badel, J. Qiu, and T. Nakano, "A new simple asymmetric hysteresis operator and its application to inverse control of piezoelectric actuators," *IEEE transactions on ultrasonics, ferroelectrics, and frequency control*, vol. 55, no. 5, 2008.
- [7] K. Kuhnen, "Modeling, identification and compensation of complex hysteretic nonlinearities: A modified prandtl-ishlinskii approach," *European journal of control*, vol. 9, no. 4, pp. 407–418, 2003.
- [8] A. Badel, J. Qiu, and T. Nakano, "Self-sensing force control of a piezoelectric actuator," *IEEE transactions on ultrasonics, ferroelectrics, and frequency control*, vol. 55, no. 12, 2008.
- [9] M. Celanovic, "A lumped parameter electromechanical model for describing the nonlinear behavior of piezoelectric actuators," *Journal of dynamic systems, measurement, and control*, vol. 119, p. 479, 1997.
- [10] R. S. Sepehr Zarif Mansour, "Design of a test setup to independently vary displacement and force of piezoelectric stack actuators," in *DOI:10.1109/ICSENS.2017.8234192*.